ULTRASONIC DETERMINATION OF ELASTIC CONSTANTS FROM OBLIQUE ANGLES OF INCIDENCE IN NON-SYMMETRY PLANES

R. B. Mignogna

Mechanics of Materials Branch
Naval Research Laboratory
Washington, DC 20375-5000

INTRODUCTION

The most common technique to determine the elastic constants of anisotropic materials from ultrasonic wave speed measurements requires that the material be cut into samples such that particular symmetry directions can be accessed for normal incidence wave speed measurements.[1,2] This is a destructive technique and is not feasible for thin or inhomogeneous materials. A truly nondestructive technique is needed. Recent work along these lines has addressed composite materials using ultrasonic immersion techniques.[3-7] However these methods have been limited to measurements in symmetry planes. Due to this limitation, all of the elastic constants can not be obtained by this technique alone. Two of the limiting factors are: the lack of a general analytic closed form solution for elastic wave propagation in anisotropic materials and that the energy vector does not, in general, lie in the plane formed by the incident wave and the refracted phase velocity. However, general analytic closed form solutions have been recently reported, removing the first of the limitations.[8,9] The second limitation greatly complicates the analysis of the problem.

The purpose of the work described here is to show that, although the actual path of the wave is along the energy vector, only the phase vector needs to be considered for the analysis of time of flight measurements in certain immersion techniques. This greatly simplifies both the time of flight measurement and analysis. In addition, the number of parameters that need to be measured for determining the elastic constants of anisotropic materials is also reduced. No assumptions are made in regard to the symmetry of the material in the analysis that follows, thus the results will be valid for any symmetry class. This removes the second limitation described above. A method for determining all of the elastic constants for anisotropic materials from wave speed measurements at oblique angles of incidence in non-symmetry planes will be discussed.

DESCRIPTION OF THE IMMERSION TECHNIQUE

The immersion technique that will be described is shown schematically in Fig.1 and is similar to those described by Markham[3], Smith[4], Kline[5] and Pearson and Murri[6]. A 'plate-like' (front and back surfaces are parallel) sample of the material is immersed in a fluid media. A transmitter and receiver transducer are placed on opposite sides of the

Review of Progress in Quantitative Nondestructive Evaluation, Vol. 9
Edited by D.O. Thompson and D.E. Chimenti
Plenum Press, New York, 1990

sample for 'pitch-catch' operation. An assumption is made here that we have an "extended" receiver, i.e., either a large array receiver or a receiver that will be scanned over an area. The receiver is represented in Fig. 1a as the rectangle labelled, "receiver". The two transducers are separated by a distance D, large enough so that the specimen normal can be positioned at arbitrary angles with respect to the direction of the sound beam (labelled incident beam). In addition, the normal of both transducers must be parallel. A set of orthogonal axes are defined with respect to the material plate such that the x_3 axis is normal to the plate. No other restrictions are placed on the axes.

Because of the fluid media, the incident beam will be a longitudinal wave. At the fluid/solid interface (I, in Fig. 1a), reflection and transmission will occur. For arbitrary angles of incidence, in general, three wave modes will be generated in the material, one quasi-longitudinal and two quasi-shear waves. The phase vectors of these waves will obey Snell's law. In general, the phase vector and corresponding energy vector of each of these waves will not be co-linear and the three energy vectors will not be co-planar. Upon impinging on the solid/fluid interface (II) reflection and transmission of each of the three wave modes will occur. The positions that the waves impinge on interface II are determined by the energy vectors. The transmitted waves at interface II emerge from these positions parallel to the incident beam (again by Snell's law). (For this discussion, we are interested only in the transmitted waves.) In general, three waves will be transmitted into the fluid. The positions where these waves impinge on the receiver will not be co-linear, as illustrated in Fig. 1a.

Four "assumptions" are used for the analysis that follows. The first is that the incident beam (phase vector), plate normal (x_3 axis) and refracted waves (phase vectors) lie in the same plane.[1] The second invokes Snell's law such that $\sin(\theta_i)/Vw = \sin(\theta_r)/Vp$, where θ_i is angle of incidence and θ_r the angle of refraction, both with respect to the x_3 axis, Vw and Vp are the phase velocities in water and in the material respectively (Vp represents any wave mode). The direction cosines n_i and n_r, are defined such that $n_i = \cos(\theta_i)$ and $nr = \cos(\theta_r)$. The third assumption is $Vg = Vp/\cos(\psi)$, where Vg is the energy or group velocity and ψ is the angle of deviation of the energy vector from the phase vector. (Vw, Vp and Vg are magnitudes only. The fourth assumption is that the exit beams from the material at interface II are parallel to the incident beam (this is actually a consequence of Snell's law and the parallel plate geometry).

The implications of the third assumption are that the magnitude of energy vector is the slant height of a right circular cone whose height (or altitude) is the magnitude of the phase vector. The axis of the cone is in the direction of the phase vector. Thus, If the phase vector is known, all possible directions of the energy vector are known but the its specific direction is not known. This is shown schematically in Fig. 1b. The plane shown intersecting the material plate in Fig. 1b is the plane formed by the incident beam (phase vector), the plate normal and the refracted phase vectors. We will henceforth refer to this plane as $\bar{V}w x \bar{V}p$. Although three wave modes may be generated, only one is depicted in Fig. 1b for clarity. The phase vector in the material is labelled $\bar{V}p$. The energy vector impinges on interface II somewhere on the perimeter of the crossed hatched area. The perimeter of the cross hatched area is an ellipse. The cross hatched area has been used to highlight the region of interface II but does not indicate other positions of the energy vector. Two of the possible energy vector paths, $\bar{V}g$, are shown where the plane $\bar{V}w x \bar{V}p$ intersect the cone. Only one of the paths is labelled in Fig. 1b.

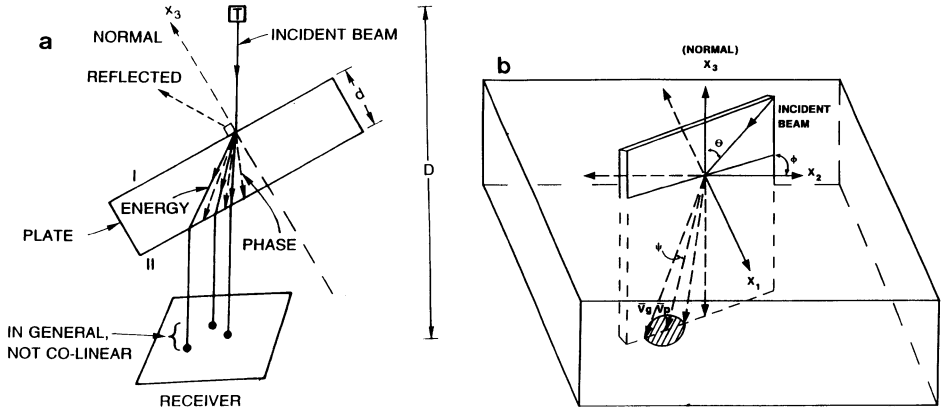

Fig. 1. a) Schematic diagram of the immersion system. b) "3-dimensional" diagram of the plate, refracted phase vector and cone of possible energy vectors (showing only one wave mode).

Figure 2a is a more detailed drawing of the plane defined by phase vectors and plate normal ($\bar{V}wx\bar{V}p$). Two of the possible energy vector paths are labelled $\bar{V}g^+$ and $\bar{V}g^-$. The "+" will be used to indicate a possible energy path that lies on any part ellipse to the left of a normal to the plane $\bar{V}wx\bar{V}p$ located at point P. The "-" will be used to indicate a possible energy path that lies on any part of the ellipse to the right of this normal. It should be noted that $Vg^+ = Vg^-$.

Although the actual path of the wave is along the energy vector, only the phase vector needs to be considered for the analysis of the time of flight measurements in this immersion techniques. What we will show is that the time of flight along the energy vector and its accompanying fluid path is equivalent to the hypothetical time of flight along the phase vector and its accompanying fluid path.

In order to show that the time of flight is the same by either path (phase vector or any possible energy vector), the problem will be broken down into four sections. Section I and II will be for the two possible energy vectors that lie in the plane $\bar{V}wx\bar{V}p$. Section I will consider $\bar{V}g^-$ and Section II, $\bar{V}g^+$. These two energy vectors are the extreme cases but set the frame work for Sections III and IV. Section III will consider all other possible energy vectors on the right (-) half of the ellipse and Section IV will consider those on the left half (+) of the ellipse. Sections I and II will refer to Fig. 2b. Figure 2b is similar to Fig. 2a but has the points (upper case letters), angles (lower case letters) and travel times ($\Delta Ts'$) labelled that will be used throughout Sections I and II. Points having a (+) or (-) correspond to $\bar{V}g^+$ and $\bar{V}g^-$, respectively. The times of flight in the material along $\bar{V}p$, $\bar{V}g^+$ and $\bar{V}g^-$ are ΔTp, ΔTg^+ and ΔTg^-, respectively. The times of flight for paths in the fluid media, as shown in Fig. 2b, are ΔTw^+ and ΔTw^-. It must be remembered through out this discussion that the magnitude of the energy velocity is the same for all possible energy vectors for a particular phase vector and deviation angle ψ for which assumption three is true.

SECTION I

In this and the following three sections, all of the discussion will be in terms of times of flight represented either directly by a time of flight or by a path length divided by the appropriate velocity. For the first

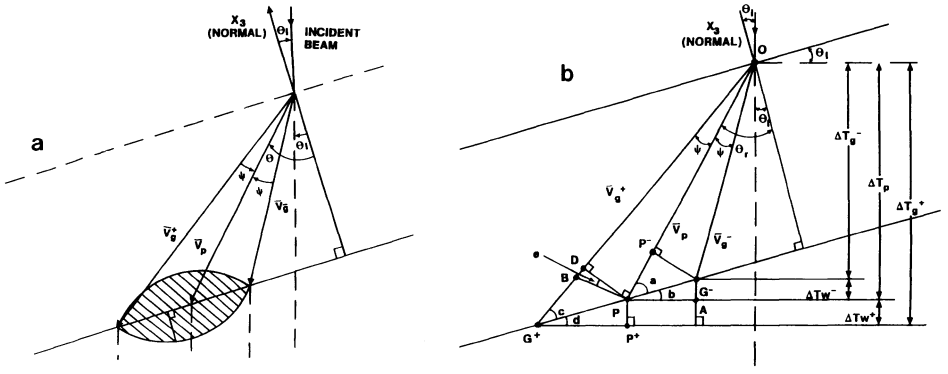

Fig. 2. a) A more detailed view of the $\bar{V}w x \bar{V}p$ plane. b) $\bar{V}w x \bar{V}p$ plane with points and angles used in Section I and II labelled. The angles are: $a = \pi - \theta_r$, $b = \theta_i$, $c = \pi - \psi - \theta_r$, $d = \theta_i$, and $e = \psi$.

case we consider the time of flight along the phase vector $\bar{V}p$ from point O to point P and the time of flight along the energy vector $\bar{V}g^-$ from point O to the point G^- and then transmitted through the fluid to point A. If the two times of flight are equivalent, we may write (making use of Fig. 2b)

$$\Delta Tp = \Delta Tg^- + \Delta Tw^- \tag{1}$$

Since,

$$\Delta Tp = OP^-/Vp + P^-P/Vp, \tag{2}$$

P^-G^- is perpendicular to OP, using the third assumption gives

$$\Delta Tg^- = OG^-/Vg^- = OP^-/[(Vg^-)\cos(\psi)] = OP^-/Vp. \tag{3}$$

$$P^-P/Vp = [(PG^-)\cos(a)]/Vp = [(PG^-)\sin(\theta_r)]/Vp \tag{4}$$

$$\Delta Tw^- = G^-A/Vw = [(PG^-)\sin(b)]/Vw = [(PG^-)\sin(\theta_i)]/Vw \tag{5}$$

using the second assumption and Eqs. 4 and 5 gives,

$$\Delta Tw^- = P^-P/Vp. \tag{6}$$

Substituting Eqs. 2,3 and 6 into Eq. 1 shows that Eq. 1 is true and therefore the time of flight is equivalent for both paths.

SECTION II

In the second case we consider the time of flight along the energy vector $\bar{V}g^+$ from point O to point G^+ and the time of flight along the phase vector $\bar{V}p$ from point O to the point P and then hypothetically transmitted through the fluid to point P^+. Again using Fig. 2b, if these two times of flight are equal, this may be written as

$$\Delta Tp + \Delta Tw^+ = \Delta Tg^+. \tag{7}$$

Since

$$\Delta Tg^+ = (OG^+)/Vg^+ = OB/Vg^+ + (BG^+)/Vg^+, \tag{8}$$

and PB is perpendicular to OP, using the third assumption gives

$$OB/Vg^{+} = OP/[(Vg^{+})\cos(\psi)] = OP/Vp = \Delta Tp. \quad (9)$$

We must now check if ΔTw^{+} equals BG^{+}/Vg^{+}.

$$BG^{+}/Vg^{+} = (DG^{+})/Vg^{+} - DB/Vg^{+} \quad (10)$$

$$DG^{+}/Vg^{+} = [(G^{+}P)\cos(c)]/Vg^{+} = [(PP^{+})\sin(\psi + \theta_r)]/[(Vg^{+})\sin(d)]$$

$$= [(PP^{+})\sin(\psi + \theta_r)]/[(Vg^{+})\sin(\theta_i)]. \quad (11)$$

DP is perpendicular to OG^{+}, therefore,

$$DB/Vg^{+} = [(DP)\tan(e)]/Vg^{+} = [(G^{+}P^{+})\sin(c)\tan(\psi)]/Vg^{+}$$

$$= [(PP^{+})\cos(\psi + \theta_r)\tan(\psi)]/[(Vg^{+})\sin(\theta_i)]. \quad (12)$$

Substituting Eqs. 11 and 12 into Eq. 10 and and expanding the sine and cosine terms yields

$$BG^{+}/Vg^{+} = [(PP^{+})\sin(\theta_r)]/[(Vg^{+})\sin(\theta_i)\cos(\psi)]$$

$$= [(PP^{+})\sin(\theta_r)]/[(Vp)\sin(\theta_i)]. \quad (13)$$

Using the second assumption, Eq. 13 becomes

$$BG^{+}/Vg^{+} = (PP^{+})/Vw = \Delta Tw^{+} \quad (14)$$

Substituting Eqs. 8, 9 and 14 into Eq. 7 shows that Eq. 7 is true and therefore the times of flight for both paths are equivalent. In addition, adding ΔTw^{+} to both sides of Eq. 1 indicates that the total time of flight or travel time from point O to the line $G^{+}P^{+}$ is the same for the path along $\bar{V}g^{+}$, $\bar{V}g^{-}$ or $\bar{V}p$.

SECTION III

The energy vector paths that will be considered in this Section and Section IV do not lie in the plane $\bar{V}w x \bar{V}p$. As mentioned earlier, the intersection of the cone $Vg = Vp/\cos(\psi)$ with interface II is an ellipse. Since the plane $\bar{V}w x \bar{V}p$ contains the plate normal and the ellipse lies in the second surface of the plate, the normal projection of the ellipse onto plane $\bar{V}w x \bar{V}p$ will be the line $G^{+}G^{-}$ of Fig. 3a. The normal projection of any energy vector that is out of the plane will be a line from point O to a point on the line $G^{+}G^{-}$ somewhere between G^{+} and G^{-}. This Section will consider all energy vectors whose projections intersect $G^{+}G^{-}$ between point G^{-} to and including P. We label the point of intersection G'^{-}. The point S is the intersection of OG'^{-} and $P^{-}G^{-}$. The angle between OP and OG'^{-} is ψ'. We will call the projected velocity along the line OG'^{-}, Vg'^{-}.

The right half of the projected base of a right circular cone formed by rotating OG^{-} about OP^{-} is coincident with $P^{-}G^{-}$. Since the magnitude of the energy velocity is the same for any possible slant height on the cone, the time that it takes to travel from O to G^{-} is the same as the time from O to S, i.e.,

$$\Delta Tg^{-} = (OG^{-})/(Vg^{-}) = OS/(Vg'^{-}). \quad (15)$$

An additional relation for OS

$$OS = (OP^{-})/\cos(\psi') \quad (16)$$

and for OG^- is

$$OG^- = (OP^-)/\cos(\psi). \tag{17}$$

From Eqs. 16 and 17 we have,

$$OS/OG^- = \cos(\psi)/\cos(\psi'). \tag{18}$$

The procedure that follows is identical to that of Section I except for the use of Eqs. 15-18. As before, if the times of flight along the two paths are equivalent, we may write

$$\Delta Tp = \Delta Tg'^- + \Delta Tw'^-. \tag{19}$$

$$\Delta Tp = (OP'^-)/Vp + (P'^-P)/Vp \tag{20}$$

$$\Delta Tg'^- = (OG'^-)/(Vg'^-) \tag{21}$$

using Eqs. 15 and 18 with Eq. 21 yields

$$OG'^-/Vg'^- = [(OG'^-)(OG^-)]/[(Vg^-)\ (OS)]$$

$$= [(OG'^-)\cos(\psi')]/[(Vg^-)\cos(\psi)]. \tag{22}$$

Using $OP'^- = (OG'^-)/\cos(\psi')$ and the third assumption in Eq. 22 gives

$$\Delta Tg'^- = (OP'^-)/Vp. \tag{23}$$

Now

$$P'^-P/Vp = [(PG'^-)\cos(a)]/Vp = [(PG'^-)\sin(\theta r)]/Vp \tag{24}$$

$$\Delta Tw'^- = (G'^-A'^-)/Vw = [(PG'^-)\sin(b)]/Vw = [(PG'^-)\sin(\theta_i)]/Vw \tag{25}$$

using the second assumption with Eq. 25 gives

$$\Delta Tw'^- = (P'^-P)/Vp \tag{26}$$

Thus Eqs. 20, 23 and 25 show that Eq. 19 is true. In other words, any path from point O, whose projection intersects the line PG^-, takes the same amount of time to traverse to the plane which is perpendicular to the incident beam (at point O) and contains the line G^+P^+.

SECTION IV

Following the same reasoning of Section III, this Section will consider all energy vectors whose projections intersect G^+G^- between point P and G^+. We label the point of intersection G'^+. The points D' and B' are the intersection of OG'^+ with both PD and PB, respectively. The angle between OP and OG'^+ is ψ' as shown in Fig 3b. We will call the projected velocity along the line OG'^+, Vg'^+.

The right half of the projected base of a right circular cone formed by rotating OG+ about OP is coincident with PB. Since the magnitude of the energy velocity is the same for any possible slant height on the cone, the time that it takes to travel from O to B is the same as the time from O to B', i.e., $OB/Vg^+ = OB'/(Vg'^+)$ or

$$Vg'^+ = [(OB')\ (Vg^+)]/OB. \tag{27}$$

Since $OB' = OP/\cos(\psi')$ and $OB = OP/\cos(\psi)$, we have

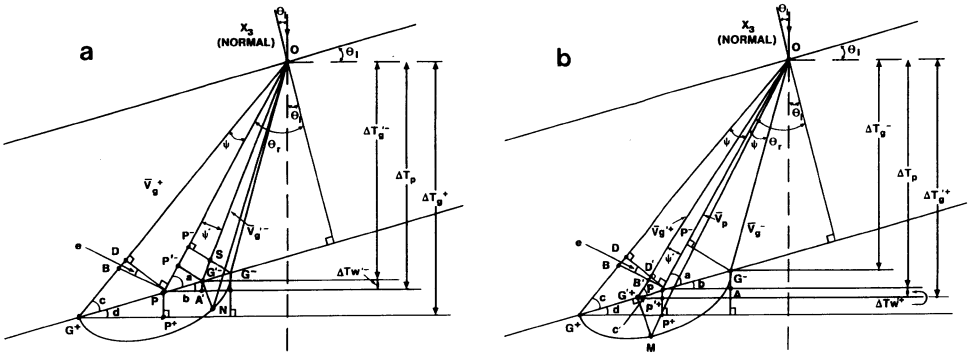

Fig. 3 $\bar{V}wx\bar{V}p$ plane showing out of plane energy vectors. a) Points and angles used in Section III, the angles are: $a = \pi - \theta_r$, $b = \theta_i$, $c = \pi - \psi - \theta_r$, $d = \theta i$, and $e = \psi$. b) Additional angles used in Section IV are $c' = \pi - \psi' - \theta_r$ and $e' = \psi'$ (not shown).

$$OB'/OB = \cos(\psi)/\cos(\psi'). \tag{28}$$

If the times of along the energy vector and and phase vector path are equivalent, we may write

$$\Delta Tp + \Delta Tw'^{+} = \Delta Tg'^{+} \tag{29}$$

where

$$\Delta Tg'^{+} = (OG'^{+})/(Vg'^{+}) = OB'/(Vg'^{+}) + (B'G'^{+})/(Vg'^{+}) \tag{30}$$

and using the third assumption

$$OB'/Vg'^{+} = OB/(Vg^{+}) = OP/[(Vg^{+})\cos(\psi)] = OP/Vp = \Delta Tp. \tag{31}$$

Does $\Delta Tw'^{+} = B'G'/(Vg'^{+})$?

$$B'G'/Vg'^{+} = D'G'/(Vg'^{+}) - D'B'/(Vg'^{+}) \tag{32}$$

$$\begin{aligned} D'G'/Vg'^{+} &= [(PG'^{+})\cos(c')]/(Vg'^{+}) \\ &= [(PP'^{+})\cos(\pi - \psi' - \theta_r)]/[(Vg'^{+})\sin(d)] \\ &= [(PP'^{+})\sin(\psi' + \theta_r)]/[(Vg'^{+})\sin(\theta_i)] \end{aligned} \tag{33}$$

$$\begin{aligned} D'B'/Vg'^{+} &= [D'P\tan(e')]/(Vg'^{+}) = [(G'^{+}P'^{+})\sin(c')\tan(\psi')]/(Vg'^{+}) \\ &= [(PP'^{+})\cos(\psi' + \theta_r)\tan(\psi')]/[(Vg'^{+})\sin(\theta_i)] \end{aligned} \tag{34}$$

Rewriting Eq. 32 using Eqs. 33 and 34 gives

$$\begin{aligned} B'G'/Vg'^{+} &= [(PP'^{+})/[(Vg'^{+})\sin(\theta_i)]\{\sin(\psi' + \theta_r) - \\ &\quad [\sin(\psi')\cos(\psi' + \theta_r)]/\cos(\psi')\} \\ &= [(PP'^{+})\sin(\theta_r)]/[(Vg'^{+})\sin(\theta_i)\cos(\psi')] \\ &= [(PP'^{+})\sin(\theta_r)]/[(Vp)\sin(\theta_i)]. \end{aligned} \tag{35}$$

Using the third assumption with Eq. 35 gives

$$B'G'/Vg'^{+} = (PP'^{+})/Vw = \Delta Tw'^{+}. \quad (36)$$

Thus Eqs. 30, 31 and 36 show that Eq. 29 is true. In other words, any path from point O, whose projection intersects the line PG^{+}, takes the same amount of time to traverse to the plane which is perpendicular to the incident beam (at point O) and contains the line $G^{+}P^{+}$.

CONCLUSIONS AND DISCUSSION

For the immersion technique that was described, Sections I - IV have shown that the time of flight along the path of the phase vector is equivalent to the time of flight along the corresponding energy path. This is true for any symmetry class of materials. In addition, it can be shown that the magnitude of the phase velocity is the same as that previously described by Pearson and Murri[6],

$$Vp = [(\Delta t/d)^2 - (2\,\Delta t/d/Vw) + (1/Vw)^2]^{-1/2} \quad (37)$$

where d is the thickness of the material, Vw is the phase velocity in the fluid and Δt is the difference in the time of flight through the fluid path without and with the material, respectively.

Since the phase vectors lie in the plane formed by the plate normal and incident beam the direction cosines of the refracted phase velocity can be written in terms of the incident wave direction cosines as:

$$l_r = l_i[(1 - \cos^2(\theta_r)/(l_i^2 + m_i^2)]^{1/2} \quad (38)$$

$$m_r = m_i[(1 - \cos^2(\theta_r)/(l_i^2 + m_i^2)]^{1/2} \quad (39)$$

$$n_r = \cos(\theta_r). \quad (40)$$

However, we can determine the magnitude of the phase velocity from the measurement and therefore θ_r from Snells law. By substituting θ_r into Eqs. 39 - 41 we have not only the magnitude but also the direction of the phase velocity. Using this information and the general analytic closed form solution for the wave equation, presented in a previous paper[8,9], it should be possible to use a least-squares approach to determine all of the elastic constants from measurements at oblique angles. Two possible difficulties that may be encountered are: the need to guarantee a unique solution for the least squares approach and the ability to experimentally resolve the the time of flight of 2 or 3 waves (from the quasi-longitudinal and shear modes) impinging on the receiver, especially the two quasi-shear modes if there is little spatial separation[7].

REFERENCES

1. M.J.P. Musgrave, Crystal Acoustics, (Holden-Day, San Fransisco, 1970).
2. R.D. Kriz and V.V Stinchomb, Experimental Mechanics, 19, 41 (1979).
3. M.F. Markham, Composite, 1, 145 (1970).
4. R.E. Smith, J. Appl. Phys., 43, 2555 (1972).
5. R. Kline, Materials Eval., 46, 986 (1988).
6. L.H. Pearson and W.J. Murri, Rev. Prog. Quantitative NDE, Vol. 6B, Eds. D.O. Thomson and D. . Chimenti, (Plenum 1987) p. 1093.
7. B. Castagnede, J. Roux and B. Hosten, Ultrasonics, 27, 280 (1989)
8. A.G. Every, Phys. Rev. B, 22, 1746 (1980).
9. R.B. Mignogna, Rev. Prog. Quantitative NDE, Vol. 8A, Eds. D.O. Thomson and D.E. Chimenti, (Plenum 1989) p. 133.